NASA TM-77762

UNSTEADY FLOW CHARACTERISTICS
IN THE NEAR-WAKE OF A TWO-DIMENSIONAL OBSTACLE

A. Dyment and P. Gryson

NASA-TM-77762 19850007375

Translation of "Quelques Propriétés de L'Ecoulement Instationnaire Dans le Sillage Proche d'un Obstacle Bidimensional", Association Aeronautique et Astronautique de France, Technical Note no. 79-08 (AAAF-NT-79-08), 1979, pp. 1-21.

NATIONAL AERONAUTICS AND SPACE ADMINISTRATION
WASHINGTON, D.C. 20546   NOVEMBER 1984

UNSTEADY FLOW CHARACTERISTICS IN THE NEAR-WAKE OF A
TWO-DIMENSIONAL OBSTACLE. (Quelques Propriétés de
l'Écoulement Instationnaire dans le Sillage Proche
d'un Obstacle Bidimensional). A. Bryant and
J. Gryson. (Paper presented at AAAF Colloque
d'Aerodynamique Appliquee, 15th, Marseille, France,
Nov.7-9,1978). Nov.1984. 22p.

1. Report No. NASA TM-77762	2. Government Accession No.	3. Recipient's Catalog No.
4. Title and Subtitle UNSTEADY FLOW CHARACTERISTICS IN THE NEAR-WAKE OF A TWO-DIMENSIONAL OBSTACLE.		5. Report Date November 1984
		6. Performing Organization Code
7. Author(s) A. Dyment and P. Gryson		8. Performing Organization Report No.
		10. Work Unit No.
9. Performing Organization Name and Address The Corporate Word, Inc. 1102 Arrott Bldg. Pittsburgh, PA 15222		11. Contract or Grant No. NASW-4006
		13. Type of Report and Period Covered Translation
12. Sponsoring Agency Name and Address National Aeronautics and Space Administration Washington, DC 20546		14. Sponsoring Agency Code

15. Supplementary Notes   Translation of "Quelques Proprietes de l'Ecoulement Instationnaire dans le Sillage Proche d'un Obstacle Bidimensional," Association Aeronautique et Astronautique de France, Technical Note No. 79-08 (AAAF-NT-79-08), 1979, pp. 1-21 (N80-13008).

16. Abstract   This phenomenological study has the objective of describing the nature of the boundary limit for breaking down vortex emissions and of formation of alternate paths in the wake of a two-dimensional obstacle at a high Reynolds number. The experiment makes use of a high-speed visualization system which makes rapidly changing phenomena possible to track. The presentation is accompanied by an animated film which shows the phenomena in slow motion.

17. Key Words (Selected by Author(s))	18. Distribution Statement Unlimited		
19. Security Classif. (of this report) Unclassified	20. Security Classif. (of this page) Unclassified	21. No. of Pages 28	22. Price

N85-15684#

NASA-HQ

N80-13008#

SUMMARY

This study, phenomenological in character, has the principal objective of showing the influence of the nature of the boundary layer at separation on vortex emission and on the formation of alternate paths in the wake of a two-dimensional obstacle, at a high Reynolds number.

The experiment was done primarily using a high-speed visualization system which makes it possible to track the development of phenomena which change rapidly as a function of time.

The presentation is accompanied by an animated film which shows the phenomena in slow motion, using a time scale on the order of 10^4 to 10^5.

TABLE OF CONTENTS

NOTATION

H	thickness of the obstacle
L	chord of the obstacle
M	Mach number upstream
N	frequency
q	exponent defined in equation (1)
R	Reynolds number
S	Strouhal number
t	time
U	velocity upstream
u	velocity in the boundary layer or in the mixing zone
U_1	velocity outside the boundary layer or the mixing zone
V	velocity of vortex propagation on a line parallel to Ox
W	velocity of alternate path vortex structure propagation parallel to Ox
x	abscissa
y	ordinate
Γ	velocity circulation
δ_1'	thickness of isothermal displacement of boundary layer
Δt	time interval between two successive flashes
ν	kinematic viscosity
τ	duration of one visualization
θ	deviation of the outside edge of a mixing zone

Indices: e   relative to vortex emission

                 a   relative to the alternate path

                 o   relative to the end of the recirculation domains

UNSTEADY FLOW CHARACTERISTICS IN THE NEAR WAKE
OF A TWO-DIMENSIONAL OBSTACLE

A. Dyment and P. Gryson
Institute of Fluid Mechanics, Lille, France

1 - INTRODUCTION

The goal of this report is to provide some information on the   /1*
properties of the near-wake from a two-dimensional obstacle in
flow at a high Reynolds number.

A theoretical plan of the vortex emission at separations and
of the formation of alternate paths was recently proposed [1].
It satisfactorily recognizes the essence of known phenomena, but
it is valid only for laminar flow. Our intent here is to examine
how the structure of the near-wake is modified when the boundary
layer at separation is turbulent.

The problem is studied experimentally from an essentially
phenomenological point of view, using high-speed flash chain
visualizations.

The results presented concern base wakes in subsonic flow at
a high Reynolds number, on the order of 2.10^5, formed with an
obstruction.

2 - STRUCTURE OF THE WAKE AT A HIGH REYNOLDS NUMBER

We recall the essence of the theoretical results given in
[1].

---

*Numbers in the margin indicate pagination in the foreign text.

Assume a permanent incompressible flow of velocity to the far U around a flat obstacle of dimensions L. The Reynolds number R = $\frac{UL}{\nu}$ being supposedly high with respect to 1, the flow plan can be broken down into several ranges where the Navier-Stokes equations take on various limited forms (fig. 1). In particular, these equations cannot be simplified in small ranges with dimensions on the order of LR^{-q}, $0 < q < 1$, including the separation points. Outside of these Navier-Stokes ranges, the detachment surface which follows the separation is unstable, which results in vortices of frequency N_e and of circulation Γ_e.

It is shown that

$$S_e = \frac{N_e L}{U} \sim R^{2q-1} \qquad \Gamma_e \sim \nu \quad . \qquad (1)$$

These results, valid for $1/2 \leq q < 7/8$, indicate that S_e is a growing function of R and that, whatever the type of separation, Γ_e has the same order of magnitude.

For a separation on an end curve point, $q = 2/3$, where $S_e \sim R^{1/3}$. For a separation on an angular point, q is equal to $\frac{3}{2(\alpha_{CL}+2)}$ where α_{CL} is the exponent of the abscissa in a normalized expression of stream function of the boundary layer range near the separation point. The behavior of the stream function is assumed to be algebraic ([2]. If the boundary layer near the angular point is perceived to be independent of distance at this point, then $\alpha_{CL} = 0$, or $q = 3/4$ and $S_e \sim R^{1/2}$.

Under the effect of viscous diffusion, the vortices generated in the separation undergo successive agglomerations. The abscissa x_n, at which the n^e agglomeration begins, and the corresponding Strouhal number S_n are given by

$$S_n \simeq 2^{-n} S_e \quad , \quad x_n \simeq 4^{n-1} x_1 \quad , \quad x_1 \sim L R^{3-4q} \quad , \qquad (2)$$

provided that the required lengths for agglomerations are disregarded (fig. 2). The outcome of these formulas is that the agglomeration process slows down very rapidly. If the sequential agglomerations are replaced with a continuous phenomenon, then $S^2 x/L \sim R$ (fig. 3).

Concerning circulation Γ_n of the vortices resulting from the $n^{\underline{e}}$ agglomeration, one can write $\Gamma_n \simeq (2\beta)^n \Gamma_e$ where β is a weighting factor, less than 1, introduced to allow for a certain diffusion in the course of the complex agglomeration phenomenon.

The preceding results concern the initial evolution of a mixing zone. However, the flow around an obstacle presents two separations, and the vortices of the two lines formed have circulations which have opposite signs and are on the same order of magnitude as in (1). These lines meet at the end of the recirculation fields and can overlap to form an alternate path. The frequency N_a of alternate path structures depends little on R, and it is such that $S_a = \dfrac{N_a L}{U} \sim 1$. Also, the length L_o of the recirculation ranges varies little with R. As S_e is very large with regard to 1, the Strouhal S_o corresponding to L_o on the successive agglomerations curve is always notably higher than S_a. Also, circulation Γ_a of structures on the alternate path is generally on the order of UL, while circulation Γ_o of the vortices of a line at the end of the recirculation fields can be significantly smaller if the number of agglomerations is not very high. The result is that an agglomeration is necessitated by   /3 interaction between the two lines, and a length of time which increases as S_o moves away from S_a is required: this relaxation time is thus a growing function of R. Thus, at moderate R, the alternate path appears immediately, whereas at very great R it is formed far downstream.

This reasoning is valid when the state of the vortices of each line is perceivably the same at the end of the recirculation

fields. It is what takes place, in particular, for a symmetrical flow. In the opposite case, for example for flow around an aerofoil profile at a high angle of attack, the vortices of the two lines cannot be found in similar conditions when they reach the end of the recirculation fields. That being the case, the agglomeration required for alternate path formation must be more significant for one of the two lines: in general it relates to the lower line ([1]). Thus the condition of the lower line determines the velocity at which the alternate path forms.

It seems surprising that the two lines of vortices tend to form an alternate path, because that obliges them to a tremendous frequency adaptation. The underlying reason is probably that the alternate path configuration assures minimum energy dissipation in the wake.

The preceding theory assumes that the fluid is incompressible and that separations are laminar. Compressibility does not fundamentally change the phenomena described, so long as the speed of sound is not reached. This was verified by the experiment ([1]).

The problem of validating the theory when confronted, at separation, with a turbulent boundary layer is the basis for the experiments described below in 4.

3 - HIGH-SPEED VISUALIZATIONS USING FLASH SERIES

These visualizations are based on variation of the air refraction index. They are not disturbing, but they do not permit following particle movement and are only applicable at a high enough velocity. In fact, as we have already said, compression does not change the qualitative aspect of the phenomena, at least in the subsonic zone.

To see a phenomenon at one instant, it is necessary that the
observation time τ be very short with respect to the typical
duration of the phenomenon. For vortex structures on the scale
of the obstacle, it is necessary to have $\tau \ll L/U$. From
$L \sim 10^{-2}$m and $U \sim 10^{-2}$m/s comes $\tau \ll 10^{-4}$s. One can satisfy this
condition using intermittent light sources, flashes, whose
duration can be less than 10^{-6}s. Note that the order of
magnitude of τ prohibits the use of standard high-speed cameras.

To reconstruct the development of a phenomenon as a function
of time, it is necessary to use a series of images separated by
intervals of known time. This goal can be achieved using a
battery of flash bulbs and regulating the interval between two
successive flashes.

The major inconvenience of this method lies in parallax
errors. These errors are minimized by placing the flash bulb and
the receiving photographic plate far from the working section.

The experiments presented here were done in the transsonic
wind tunnel of the Institute of Fluid Mechanics at Lille. This
is a return circuit continuous-function wind tunnel. Part of the
air used is replaced by fresh air drawn from the atmosphere.
This air passes through a dryer before being introduced into the
aerodynamic system. This preparation avoids condensation and
stabilizes the air temperature in the tunnel. The working
section is 42 x 200 mm^2 in area; its lateral walls are equipped
with interferometric ports. The two other walls are formed using
sloped grates with longitudinal slots. Movable counter-grills
allow permeability to be regulated. To stabilize the flow, a
sonic throat is established by using two flaps at the exit of the
working section.

The visualizations were produced through a method developed
by the Franco-German Research Institute at Saint-Louis (I.S.L.),

which included 24 flash bulbs and (24) photographic plates. The
duration τ of each flash is around $0.3 \cdot 10^{-6}$s. The interval Δt
between two successive flashes is continuously adjustable from
one second to 10^{-7}s. The apparatus functions in shadowgraph and
also in the schlieren system by adding a plate equipped with 24
adjustable schlieren system knives.

Dimensions L of the obstacles are on the order of 10^{-2}m and
velocity U on the order of 10^{2}m/s. It is known that the periods
below which viscosity is to be considered are about $L/U\, R^{-3/4}$ /5
[3]. This is much less than the duration of the flashes, so that
visualizations do not permit accessing scales of turbulent
movement where dissipation occurs.

With the preceding data, Navier-Stokes range dimensions are
on the order of 10^{-5}m, which makes it impossible to observe
movement in these ranges. Also, for these ranges, the condition
relative to τ is not satisfied with the apparatus used. Thus, it
is not possible to observe the vortex emission nor the beginning
of agglomeration. It must also be noted that the phenomenon
observed is less simple than the schematic description given in 2
because of the kinetic velocity field induced by the vortices
emitted. Consequently, no wait is necessary to obtain very
precise quantitive results.

Observations made with smaller Δt values make it possible to
follow mixing zone vortex propagation. To determine frequency N
a given abscissa is used and time between the passage of two
successive vortices is measured. Interpolation is almost always
necessary. Since, also, the placement of vortices is not very
precise because they are not punctual, the frequency measured
constitutes only an order of magnitude. This is also true of
propagation velocity V obtained by displacing the vortices
between two successive plates.

For quantitative study of an alternate path it is necessary to use a Δt interval such that at least one period of the path is covered by the 24 plates of one sequence.

4 - INFLUENCE OF THE NATURE OF THE BOUNDARY LAYER SEPARATION

The theory summarized in 2 assumes that the flow is laminar. A priori it seems natural to consider that, in the presence of a turbulent boundary layer, the emission of vortices will remain unchanged provided that the phenomenon is produced in the viscous film of the wall.

For a flat plate boundary layer, the Reynolds number formed with the thickness of the viscous film is perceivably on the order of $R^{1/10}$. The dimensions of the Navier-Stokes range being LR^{-q}, we obtain the condition $R^{1-q} \ll R^{1/10}$, or $q > 9/10$, which is not compatible with the theory proposed in 2. It thus seems <u>/6</u> true that vortex emission is influenced by boundary layer turbulence.

To verify these hypotheses, we did experiments with models showing a fixed separation, to avoid the complications from displacing the separation when it is produced on a point of the wall where the curvature ends. It is known that this displacement is done at frequency N_a because it results from coupling with the alternate path ([1]).

Two models were tested. They are symmetrical and made up of a circular cap, pointed forward, extended by a plate of constant thickness H = 20 mm up to a straight base. In results given later, H will be taken as reference length to form representative parameters without flow dimension.

The experiment is based essentially on visualizations. At too small a Mach number, the volumetric mass variations are

insufficient to supply a sufficiently clear image of the flow.
On the other hand, if the Mach number is too high, new phenomena
appear, linked to the existence of shock waves [1]. Allowing for
these items, we chose to do the experiments at M $\simeq$ 0.6.

The velocities in the boundary layers and in the mixing zones
were determined using pitot readings. At distance H/4 upstream
from the base, the L = 70 mm chord model shows a laminar flat
plate boundary layer, and the L = 150 mm chord model shows a
turbulent boundary layer (fig. 4 and 5). The turbulent boundary
layer is thicker than the laminar boundary layer, but the ratio $\frac{\delta'_1}{H}$
is on the same order of magnitude for the two flows.

At distance H/2 downstream from the base, velocity profiles
in the mixing zones are similar. This means that, in the case of
laminar separation, the flow in the sounded section already shows
a marked turbulent character. According to the visualizations,
this section is located almost at the end of the recirculation
ranges. The result obtained shows that, from the point of view
of the average flow, the nature of the boundary layer has a
negligible effect on the wake. This property is illustrated by
the schlieren system visualizations at long exposure time, which
do not permit distinction between the two wakes (plate A).

Note that wake dimensions vary little as a function of the   /7
Mach number, contrary to other obstacles such as a normal flat
plate in the wind (plate B).

Plate C, whose photos were deliberately darkened, shows the
existence of turbulent gusts in the boundary layer of the large
model. We will see that these gusts act on the vortical
structures of the mixing zones.

High-speed visualizations by flash series were done for Δt =
2, 5, 10 and 20 μs. Plate D, for which Δt = 5 μs, makes it

13

possible to follow the development of the mixing zones vortices in the small model. Analysis gives $NH/U \simeq 8$ to 10, whereas with turbulent (plate F), values between 3.5 and 4.5 are obtained. It is not possible to discover significant variations of N as a function of the abscissa, because the mixing zones are not sufficiently extended. Also, the agglomeration phenomenon slows down rapidly, and it is strongly perturbed by interaction with the alternate path. It is stated that, in accordance with the theoretical plan, N is much larger than N_a, whose value will be given later (fig. 6). In turbulent, the vortices seem more extended and less clear than in laminar: this is because they are not purely two-dimensional, in particular due to the influence of the boundary layer gusts. The effect of the boundary layer turbulence is perfectly perceptible on the second part of plate C and on plate F.

Propagation velocity V of mixing zone vortices is not constant, as assumed in the theoretical plan, but increases as a function of the abscissa. In laminar it reaches U_1 at the end of the recirculation ranges, where the vortices coil and agglomerate to form the alternate path structures. In turbulent, the increase in V is less marked; there is an important dispersion, V being generally between $0.5U$ and U, and certain analyses reveal a periodicity equal to that of the alternate path.

Note that the vortices act as sonic emission sources. The origin of the propagation of acoustic waves generated is perfectly visible on the high-speed visualization plates.

The photography of plates E and F represents a period and a semi-period of the alternate path, in laminar and in turbulent respectively. It is stated that the two alternate paths are very close to each other. Figure 6 gives the values of $\frac{N_aH}{U}$ obtained at different Mach numbers for Reynolds numbers $\frac{UH}{\nu}$ between $1.8 \cdot 10^5$ and $8 \cdot 10^5$. We see that, in the range of the Mach-Reynolds

plan explored, $\frac{NaH}{U}$ is not very noticeable in the variations of these two parameters.

Propagation velocity W of the structures of the alternate path increases and asymptotically approaches U as distance from the obstacle increases and as the path lengthens (fig. 7). Two restorations of trajectories of vortical structures in a row are represented in figure 8: they differ very little from each other.

Examination of the set of visualizations proves the importance of the coupling between the alternate path and separations. Wake oscillation occurs at frequency N_a, with an amplitude which increases with the Mach number ([1]). Deviation θ of the outside mixing zone edge was determined from shadowgraphic plates. It is represented as a function of the time in figure 9: the coupling is more intense in the case of the laminar separation.

The difference between laminar separation and turbulent separation can be too great to disregard. The theory in 2 indicates that in laminar flow, when R increases, the alternate path is formed with more difficulty because N_o is farther from N_a. It is thus possible that, above a certain value of R, the alternate path can appear only far downstream of the recirculation ranges. This explains why, according to most experimenters, there is no alternate path at a high Reynolds number, at least near the obstacle. However, these same experimenters indicate that the wake exhibits a periodic flow when separations become turbulent. This phenomenon can be partially explained by the results obtained here. In effect, the agglomeration which produces the alternate path can take place more easily in the presence of a turbulent separation, since in this case the mixing zone vortex frequency is clearly closer to N_a than in the laminar regime.

5 - CONCLUSION

The kinetic phenomena produced in the near-wake of a two-dimensional obstacle constitute a vast subject for research, little explored as yet due to lack of experimental procedures.

The study presented here is intended to examine in what <u>/9</u> measure the structure of a wake is influenced by the nature of the separation boundary layer.

The results obtained using high-speed visualizations show that, for the Reynolds numbers considered, there exists an alternate path whether the separation is laminar or turbulent: the characteristics of the average flow and those of the alternate path are very close in the two cases. Also, the mechanism of the vortical emission at the separations does not seem to change fundamentally when the boundary layer is turbulent, but it differs from the quantitative results which apply to mixing zones which run along recirculation ranges: the Strouhal numbers and the propagation velocities of the vortices are different, as is the case for separation line oscillation amplitude. These differences can have an influence on the ease with which the alternate path is formed in the wake.

Certain properties described in this report appear more evident when projected on animated film, made from visualization plates, which recaptures the evolution of the rapidly variable phenomena with a time scale on the order of 10^4 to 10^5.

REFERENCES

[1] DYMENT and GRYSON
     Unsteady Aerodynamics
     AGARD, C.P., No. 227, 1978

[2] FRANOIS
     ONERA, Publ., No. 128, 1968.

[3] LANDAU, LIFSCHITZ
     Mécanique des Fluides (Fluid Mechanics), Moscow, 1971.

EI

NS   CL

SCL

ERC

$\vec{U}$
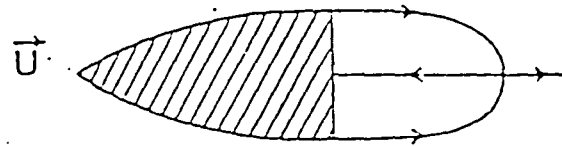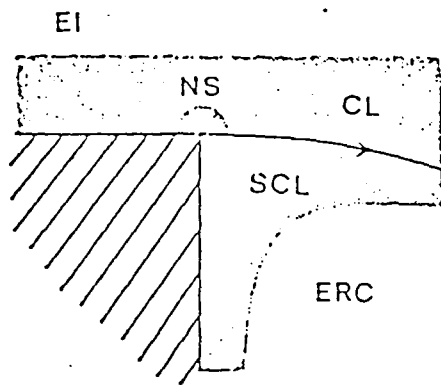
RANGES

EI	Irrotational Euler
ERC	Euler at Constant Rotation
CL	Boundary Layer
SCL	Sub-Boundary Layer
NS	Navier Stokes

Fig:1

S

S_e

S_1

S_2
S_3

0   x_1 x_2 x_3 x

Fig:2

S

S_e

S_o

S_a

L_o/L x/l

L_o

Fig:3

18
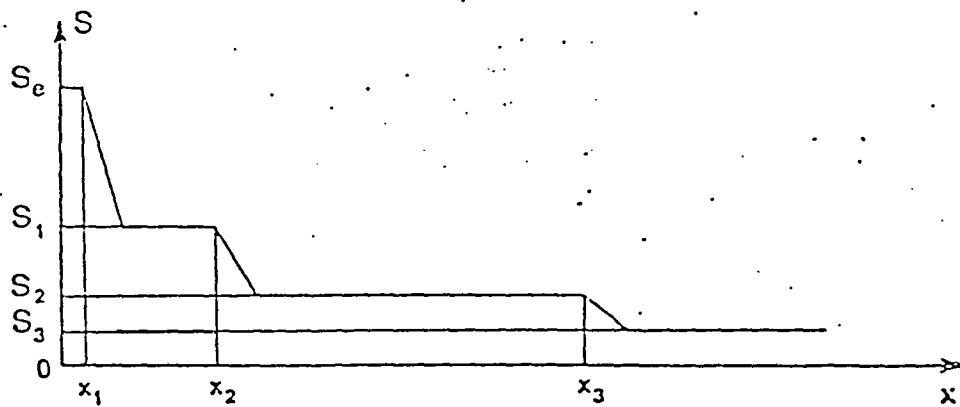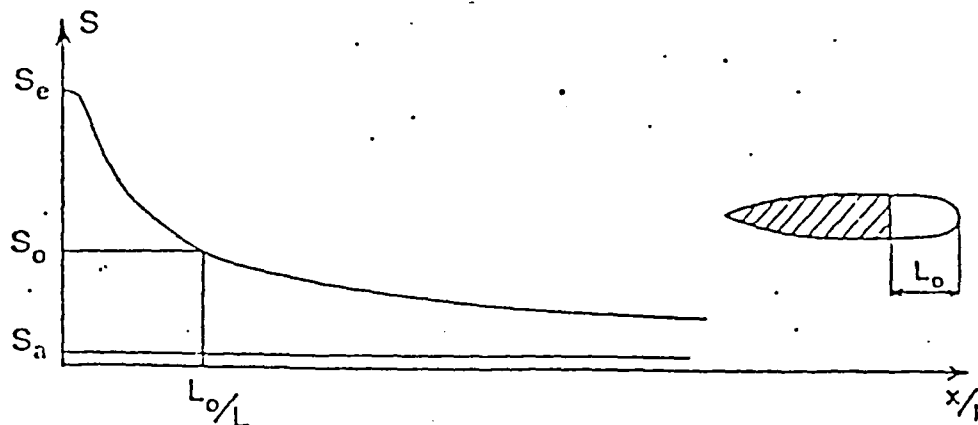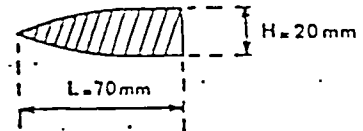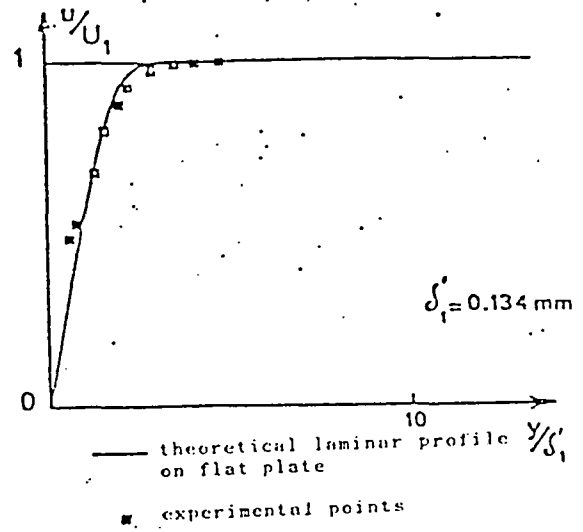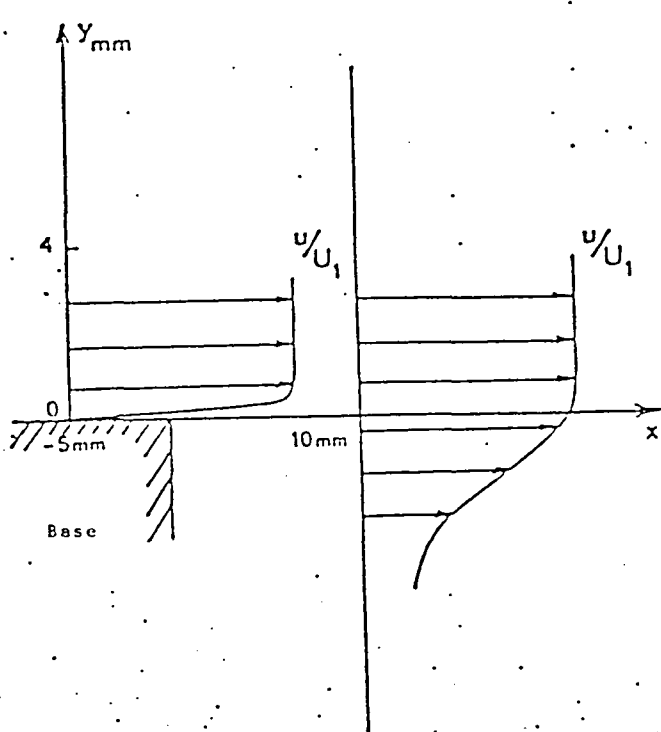
Fig:4
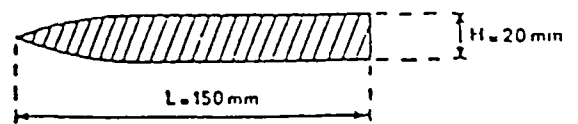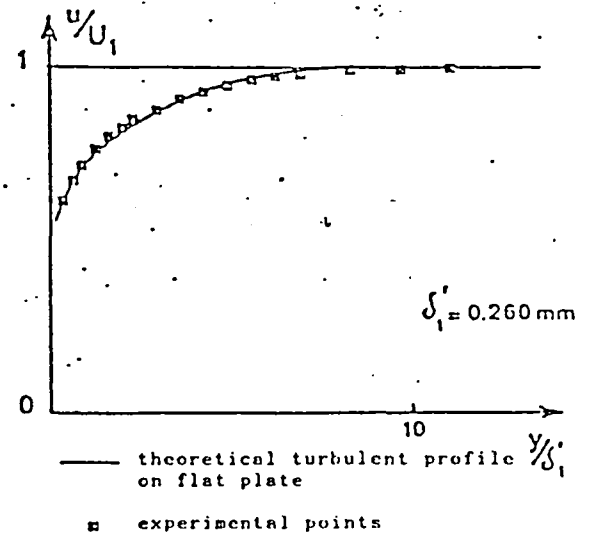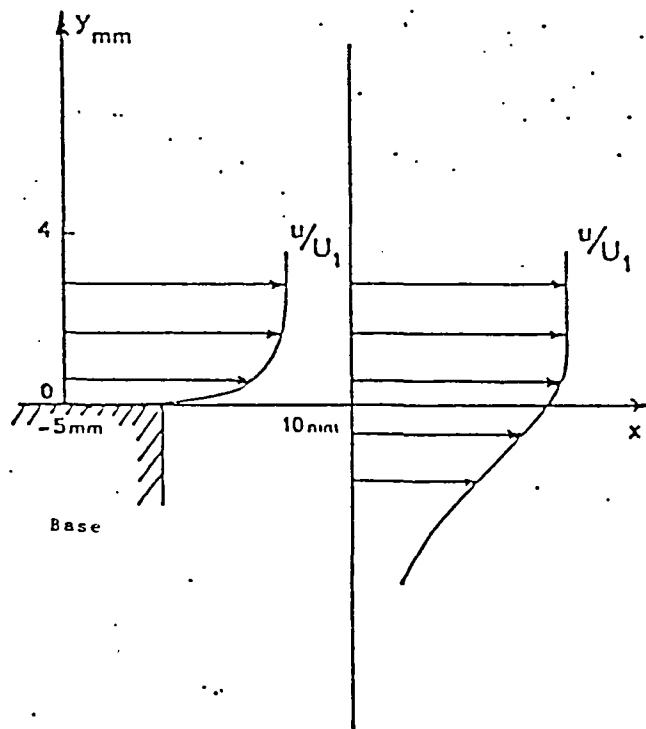
Fig:5
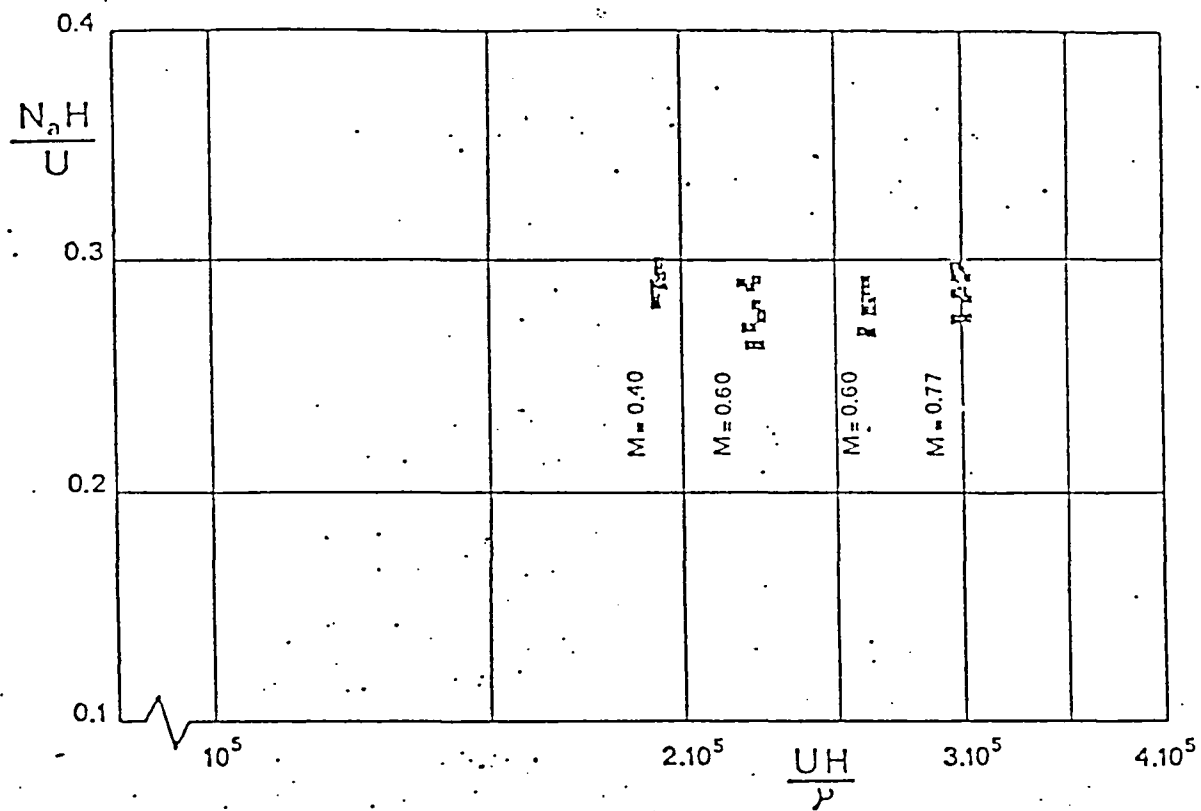
Fig:6
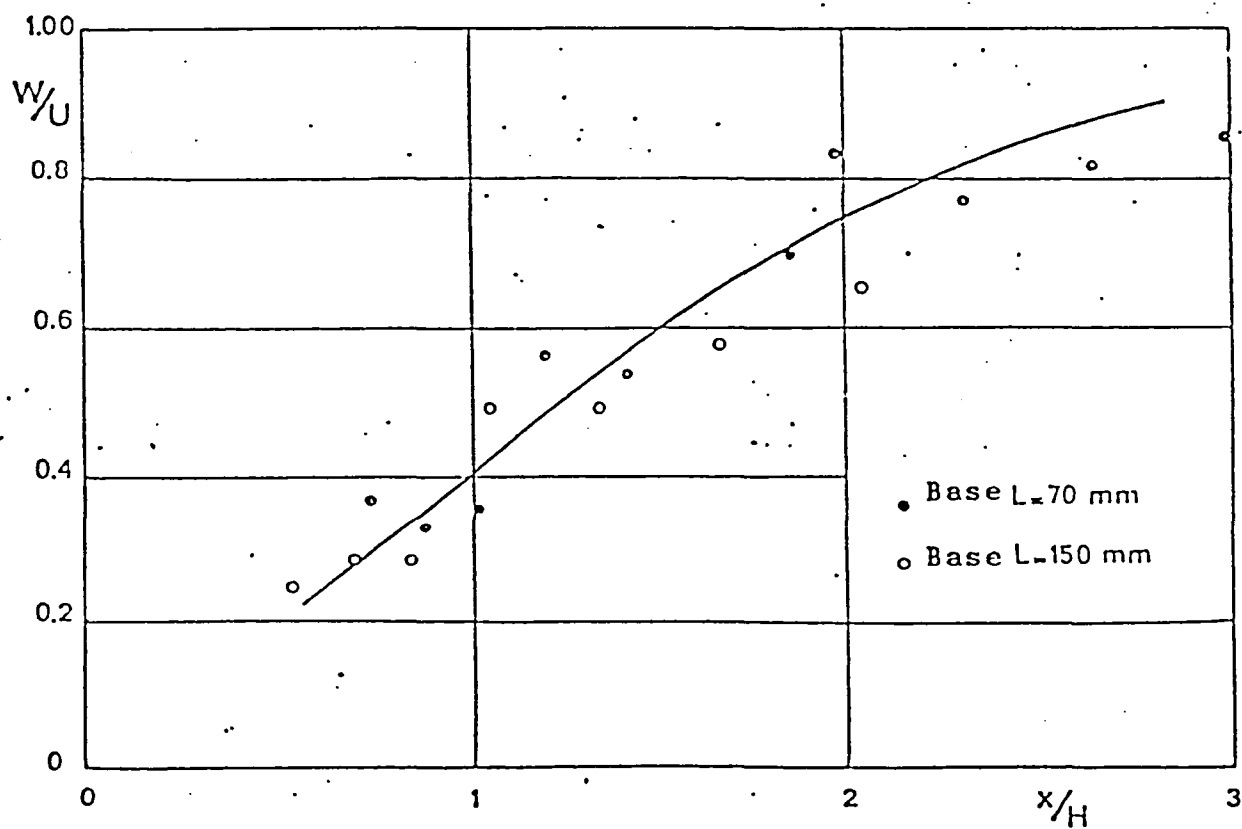
Fig:7
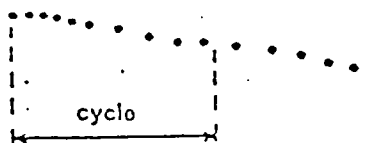
$\Delta t = 40 \mu s \qquad M = 0.60$

$H = 20 \, mm \qquad U = 204 \, m/s$

$L = 70 \, mm \qquad \dfrac{UH}{\nu} = 2.2 \, 10^{5}$

• successive positions of a vortex center
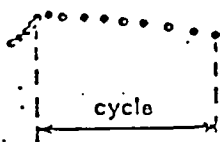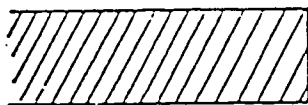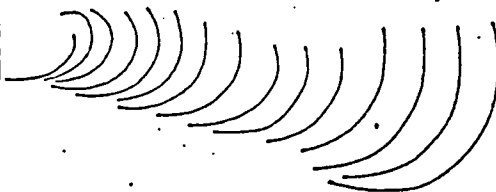
$\Delta t = 40 \mu s \qquad M = 0.60$

$H = 20 \, mm \qquad U = 203 \, m/s$

$L = 150 \, mm \qquad \dfrac{UH}{\nu} = 2.2 \, 10^{5}$

• successive positions of a vortex center
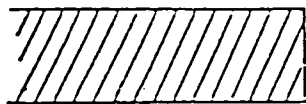
Fig : 8

$$\frac{U}{N_a H} \simeq 3.6$$
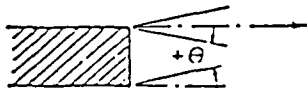
Upper vortices ○
Lower vortices ▼

$\Theta°$

12

8

4

U = 204 m/s
L = 70 mm

0   1   2   3 $\frac{U t}{H}$ 4   5

$\Theta°$

8

4

U = 203 m/s
L = 150 mm

0   1   2   3 $\frac{U t}{H}$ 4   5
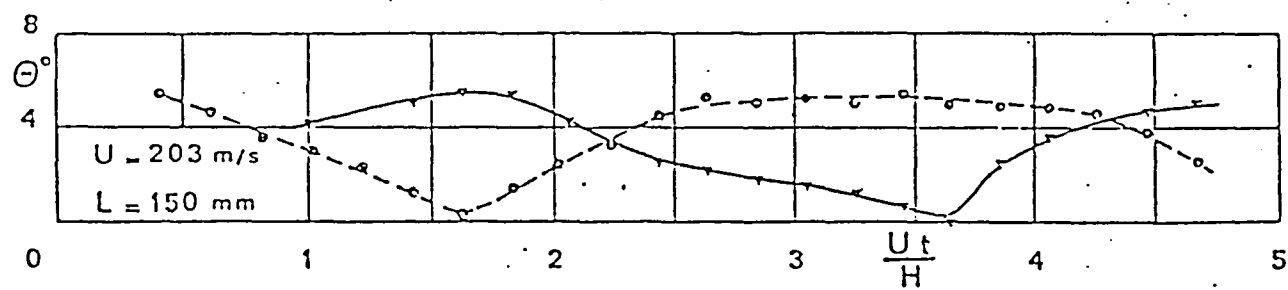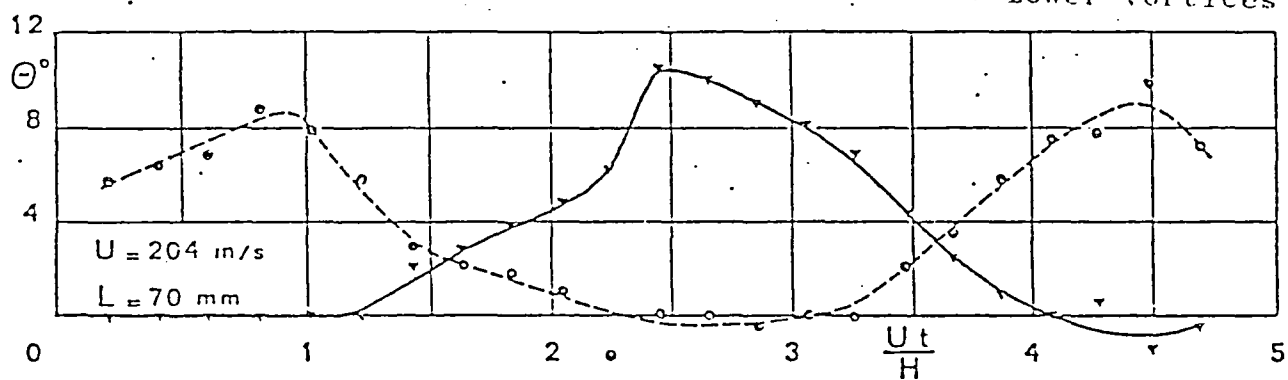
Fig:9

SCHLIEREN PHOTOGRAPHS

Exposure $= \frac{1}{400}$ s

H $=$ 20 mm

M $=$ 0.60

U $=$ 204 m/s
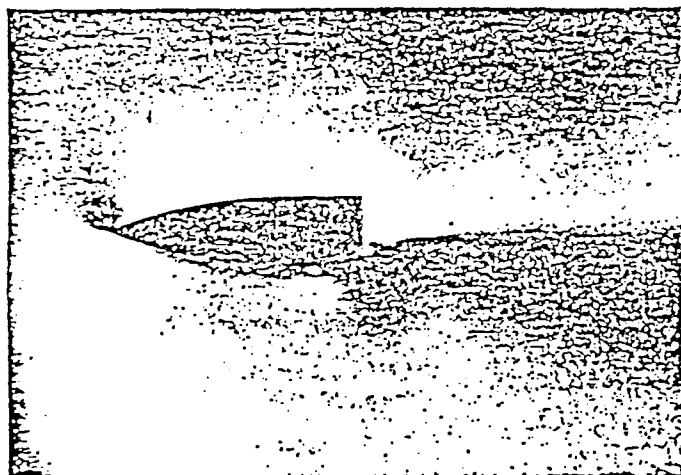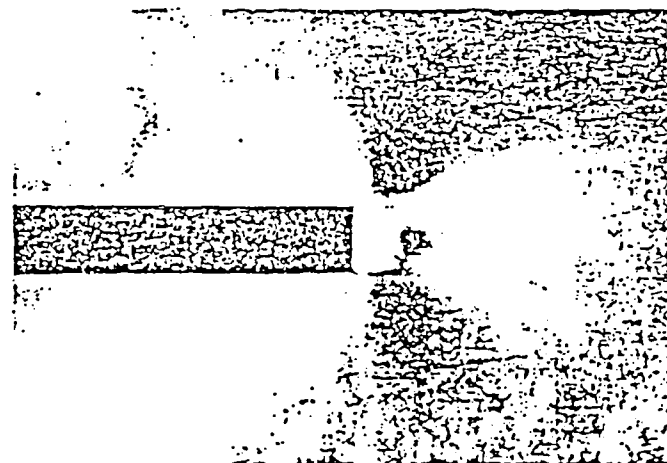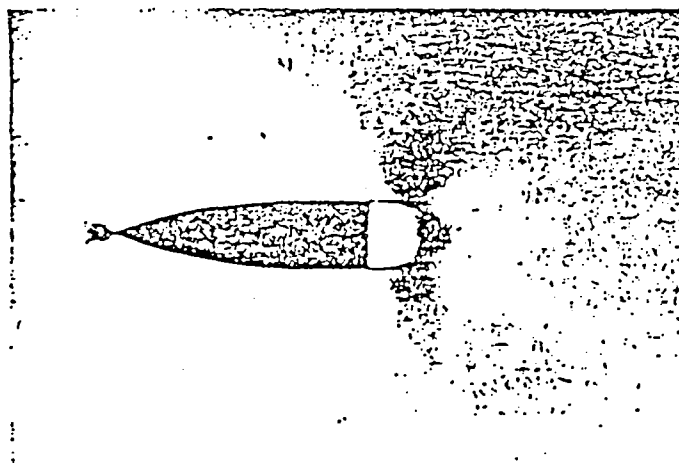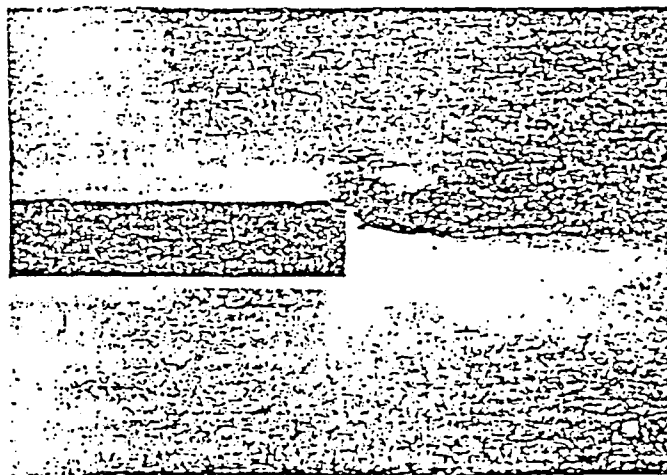
L $=$ 70 mm   L $=$ 150 mm

PLATE   BASE

H = 12 mm   H = 24 mm
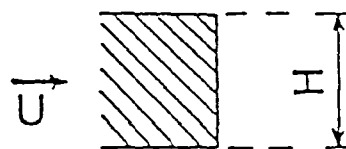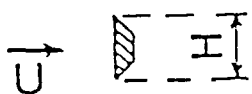
$\vec{U}$ Shadowgraphs $\vec{U}$

M = 0.30   M = 0.40

0.60   0.60

0.76   0.77

Plate C
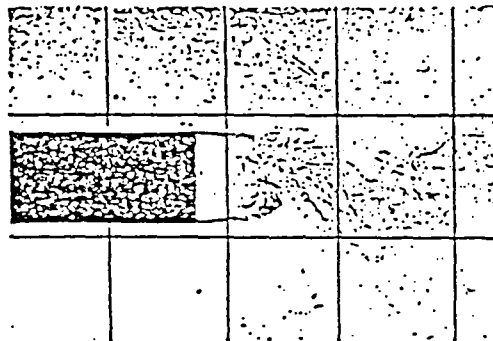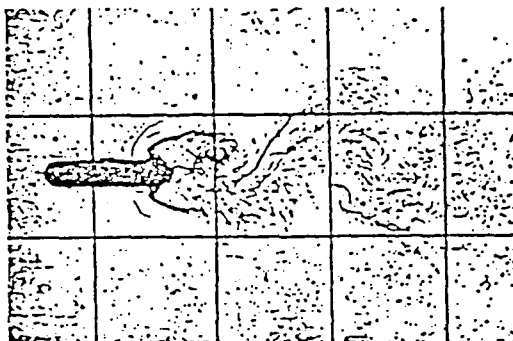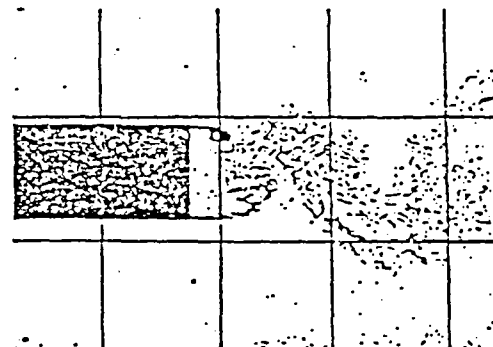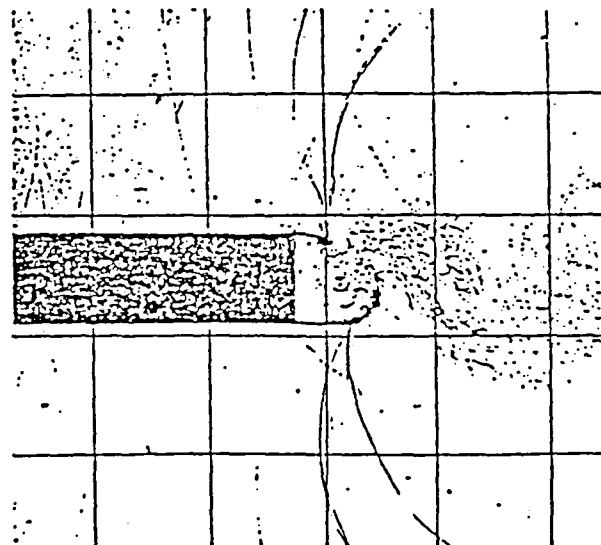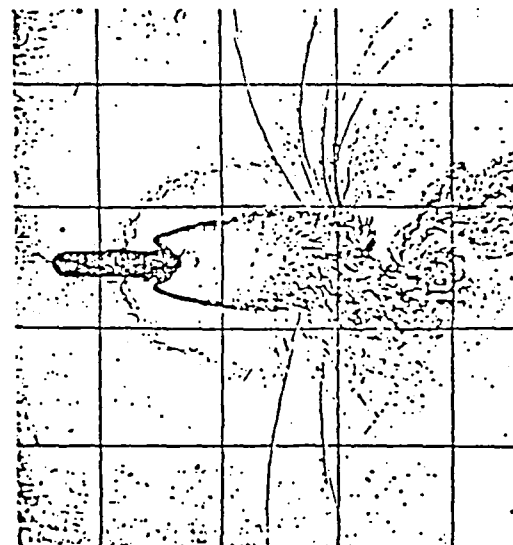
SHADOWGRAPHS

Exposure = 0.3 μs

H = 20 mm
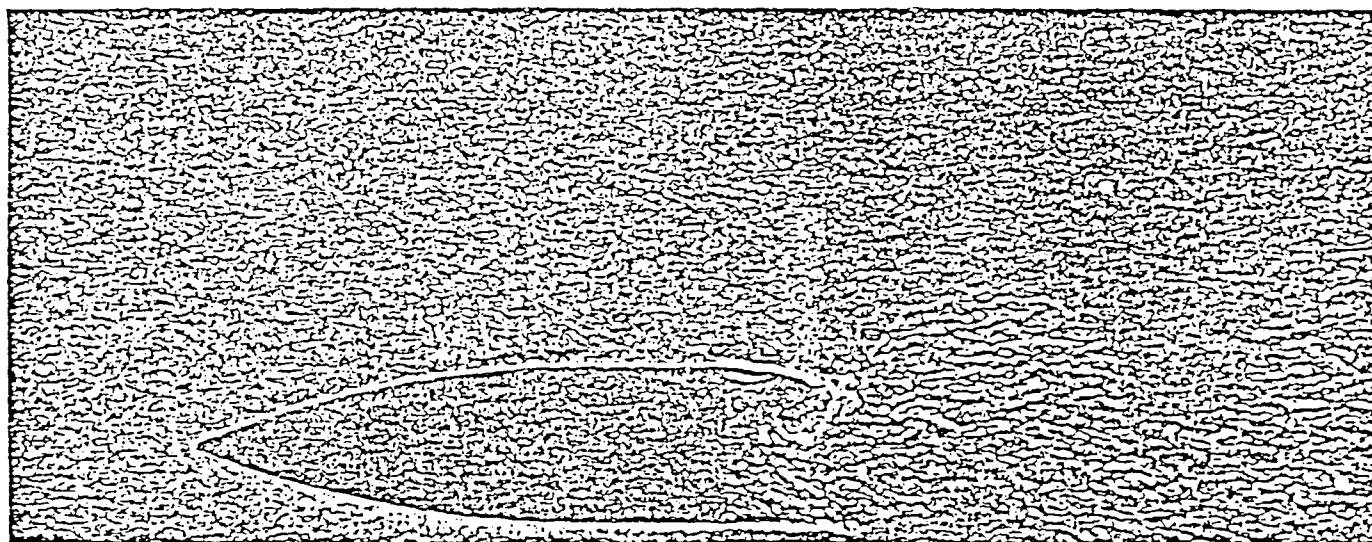
M = 0.60

U = 204 m/s
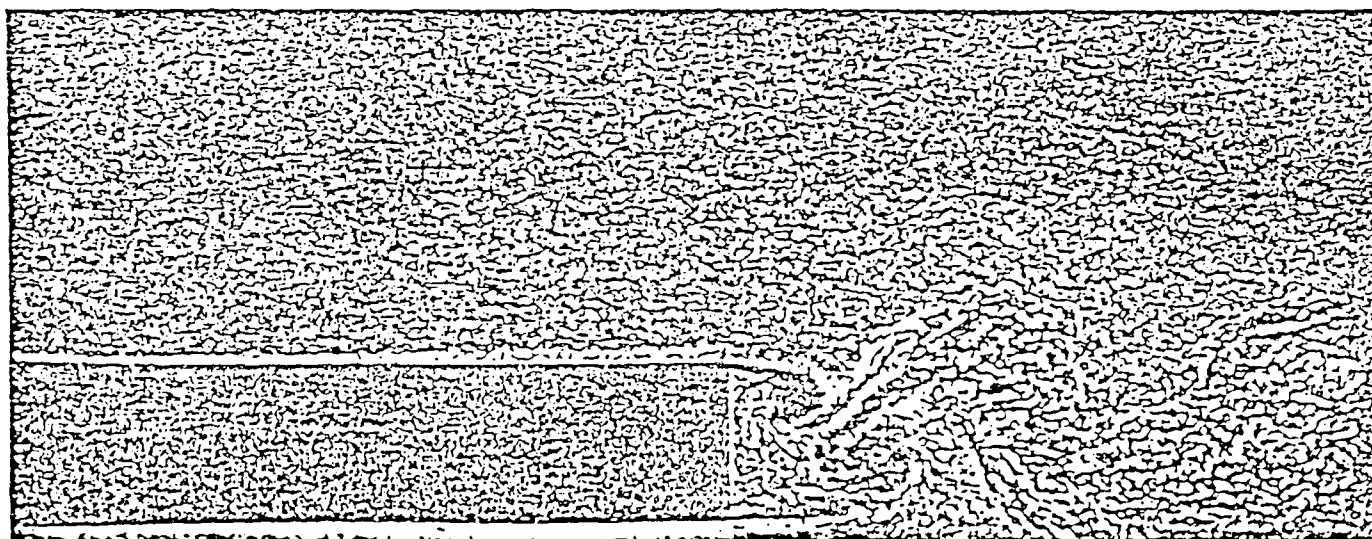
L = 70 mm

L = 150 mm

SCHLIEREN PHOTOGRAPHS

Exposure = $0.3\,\mu s$

$\Delta t = 5\,\mu s$ $\qquad\qquad$ $M = 0.60$

$H = 20\,mm$ $\qquad\qquad$ $U = 203\,m/_s$

$L = 70\,mm$ $\qquad\qquad$ $\dfrac{UH}{\nu} = 2.2\,10^5$

1

2

3
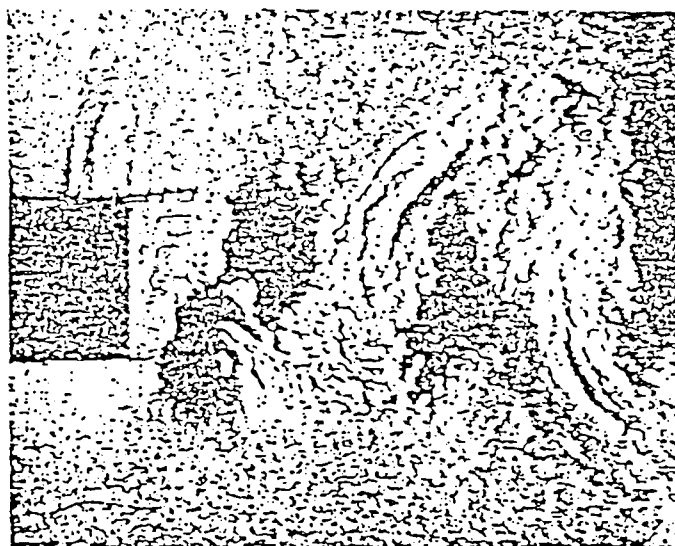
4

SCHLIEREN PHOTOGRAPHS

Exposure = 0.3 µs

$\Delta t = 80 \, \mu s$

$H = 20 \, mm$

$L = 70 \, mm$

$M = 0.60$

$U = 204 \, m/s$

$\dfrac{UH}{\nu} = 2.2 \, 10^{5}$
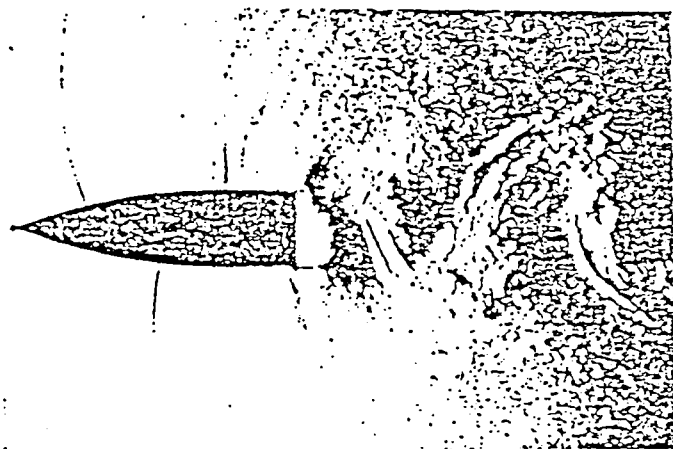
1
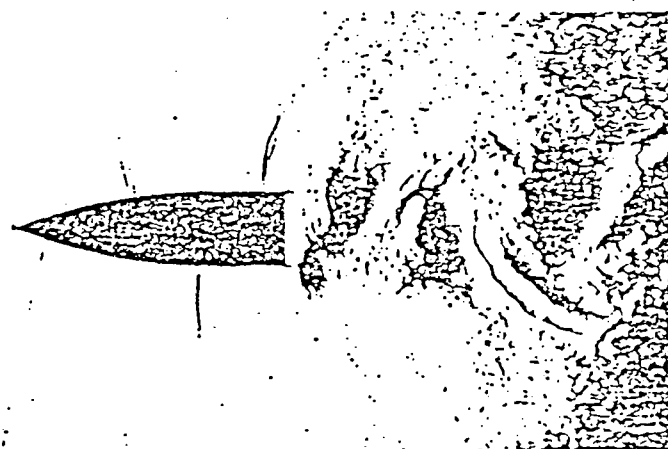
4
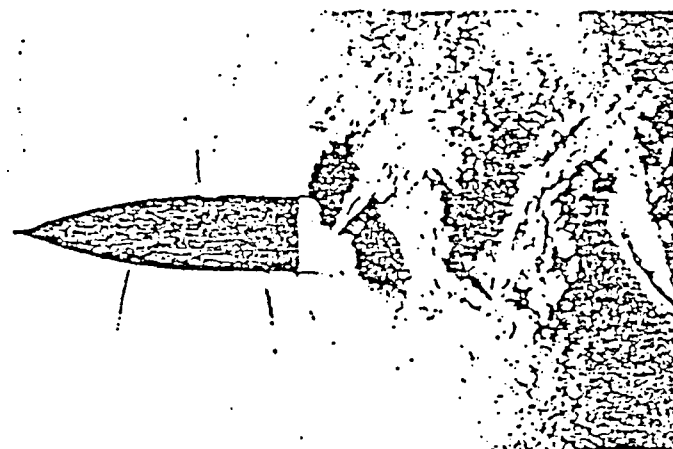
2
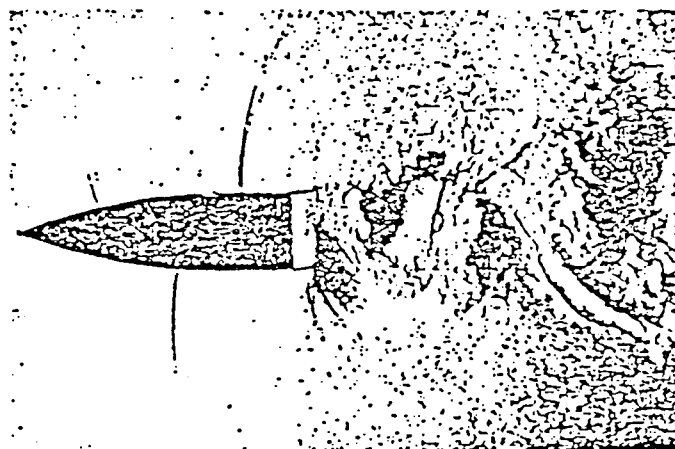
5
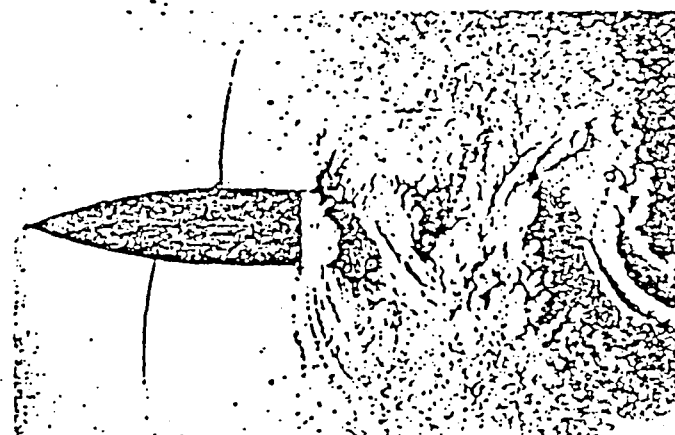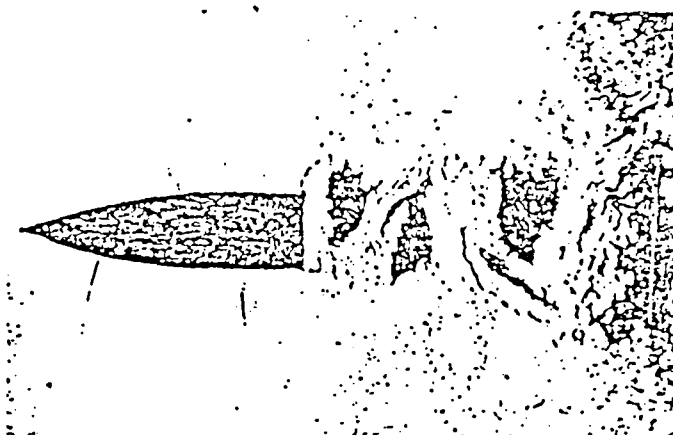
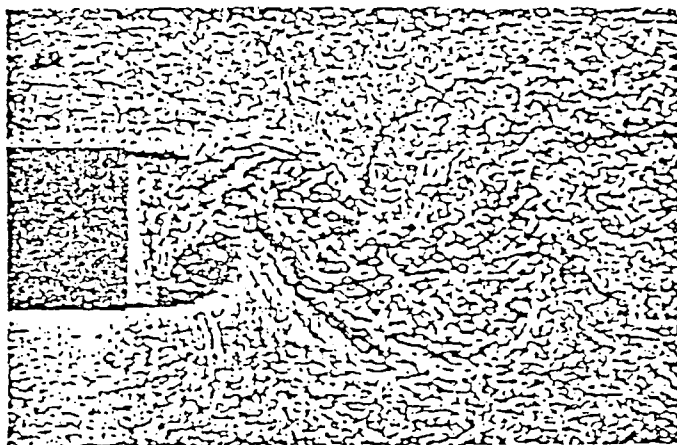# SHADOWGRAPHS

Exposure = 0.3 µs

$\Delta t = 40\,\mu s$

$H = 20\,mm$

$L = 150\,mm$

$M = 0.60$

$U = 203\ m/s$

$\dfrac{UH}{\nu} = 2.2 \cdot 10^{5}$

1

4

2

5